https://doi.org/10.5194/egusphere-2024-3954
Preprint. Discussion started: 3 February 2025

Analysis of Long-Term Changes in Extreme Waves in the Northwest Pacific Over the Past 60 Years

Yang-Ming Fan[1]

[1]Coastal Ocean Monitoring Center, National Cheng Kung University, Tainan, 701, Taiwan

Correspondence to: Yang-Ming Fan (ymfan@mail.ncku.edu.tw)

Abstract. This study analyses wave height trends in the Northwest Pacific over the past 60 years and estimates design wave heights across various return periods to assess the resilience of marine and coastal structures to extreme wave events. Design wave height is a critical parameter for evaluating structural stability and safety, especially during typhoon season (May to October), when strong winds and rapid movements often trigger extreme waves, significantly impacting offshore structures, coastlines, and ports. To avoid underestimating risks during typhoon season, this study simulated wave heights from 1961 to 2020 using historical wind field data from the EC-Earth3 climate model and the WAVEWATCH III wave model. The 95th percentile was chosen as the threshold for extreme wave events, and the Generalized Pareto Distribution (GPD) model was applied for fitting. Finally, the bootstrap resampling method was used to quantify uncertainties in return periods to ensure reliable assessments of design wave heights. The analysis shows a slight increase in design wave heights with longer return periods (10 to 200 years) near Taiwan, with significantly higher wave heights observed in the southern and eastern regions, indicating a need to enhance disaster resilience in marine infrastructure designs for these areas.

1 Introduction

Global warming has become an irreversible trend, with governments worldwide striving to mitigate its effects through carbon emission controls. Despite these efforts, the impacts of global warming can only be slowed, not entirely reversed. Since 2021, the Intergovernmental Panel on Climate Change (IPCC) has released its Sixth Assessment Report (AR6), incorporating Shared Socioeconomic Pathways (SSPs) to project various climate change scenarios. Key topics in AR6 include global temperature rise, the frequency and intensity of extreme rainfall, Arctic ice melt, and sea-level rise. Notably, the report suggests that while the frequency of tropical cyclones may decrease, their intensity is expected to increase. However, definitive conclusions regarding future wave climates remain elusive, particularly for the waters surrounding Taiwan, highlighting the need for further research.

Ocean surface waves, generated by wind, are essential variables in climate predictions (Hemer et al., 2012). They play a critical role as moderators of air-sea interactions (Cavaleri et al., 2012; Fan and Griffies, 2014; Breivik et al., 2015) and have significant implications for coastal safety, influencing coastal erosion, flooding, and the design of offshore structures and vessels. Reliable

https://doi.org/10.5194/egusphere-2024-3954
Preprint. Discussion started: 3 February 2025

wave predictions require accurate wind field estimates to drive wave models (Hemer et al., 2013; Hemer and Trenham, 2016). Alternatively, index parameters derived from observational or modelled data can serve as reference factors for wave predictions (Wang et al., 2014).

Extensive research has been conducted on global wave climates. For example, studies by Dobrynin et al. (2012), Semedo et al. (2012), Fan et al. (2013), Mori et al. (2013), Hemer et al. (2013), Wang et al. (2014), Fan and Griffies (2014), Shimura et al. (2015a), and Hemer and Trenham (2016) have provided insights into wave dynamics and variability. Regional analyses have focused on areas such as the Arctic Ocean (Khon et al., 2014), the Atlantic Ocean (Grabemann et al., 2015; Perez et al., 2015; Martınez-Asensio et al., 2016; Gallagher et al., 2016; Aarnes et al., 2017), and the Pacific Ocean (Chien et al., 2014; Erikson et al., 2015; Shimura et al., 2015b, 2016), with most relying on numerical simulations.

In the context of Taiwan, the relatively small geographic area and complex coastal dynamics necessitate high-resolution climate model data to accurately characterize wave behaviour in surrounding waters. Recent findings, such as those by the Ministry of Science and Technology (MOST, 2022), have highlighted the impacts of warming scenarios on typhoon intensity and their potential to increase coastal wave and storm surge risks. However, these projections were based on the AR5 RCP8.5 scenario (MOST, 2021), underscoring the need for updated, high-resolution projections to capture wave dynamics more effectively under changing climate conditions.

The Coupled Model Intercomparison Project (CMIP) has facilitated collaborative climate modelling by multiple international research teams, providing a comprehensive multi-model framework for understanding climate variability. The latest phase, CMIP6, supports the AR6 projections and provides data spanning from 2015 to 2100. Among the CMIP6 models, the European EC-Earth3 model has demonstrated exceptional performance in simulating atmospheric circulation in East Asia (Döscher et al., 2022; Zheng et al., 2022). EC-Earth3 provides projections for 10-meter wind speeds and sea-level pressure under SSP1-2.6, SSP2-4.5, SSP3-7.0, and SSP5-8.5 scenarios, with a spatial resolution of 100 kilometres and a temporal resolution of 6 hours.

Despite the advancements in global climate modelling, the relatively coarse resolution of these outputs limits their applicability for regional analyses, particularly in areas with intricate coastal and oceanic dynamics, such as Taiwan. Downscaling methods are therefore essential for deriving high-resolution spatial and temporal wave data. Such methods enable a more precise characterization of wave trends and their potential impacts, providing critical insights for disaster prevention and coastal resilience planning under various climate change scenarios.

2 Research Objectives and Scope

Investigating wave changes under climate change necessitates a comprehensive analysis of both historical wave data and future scenario projections (Mentaschi et al., 2017; Lemos et al., 2023; Meucci et al., 2023). Historical wave data provide critical insights into seasonal variations and long-term trends, forming the basis for understanding baseline wave behaviour. Meanwhile, future scenario projections shed light on potential wave changes under various climate change assumptions.

https://doi.org/10.5194/egusphere-2024-3954
Preprint. Discussion started: 3 February 2025

Together, these datasets are vital for assessing future risks and formulating effective strategies to address the impacts of climate change.

This study aims to develop an artificial intelligence-based wave downscaling model to produce high-resolution spatial and temporal wave data. Using this model, the research focuses on analysing the spatiotemporal changes in historical waves and evaluating design wave heights across different return periods in the Northwest Pacific, with particular attention to the waters around Taiwan. These efforts are crucial for advancing the understanding of wave changes and supporting risk assessments, infrastructure design, and adaptation planning in the context of a changing climate.

3 Data Collection and Sources

3.1 Collection of Wind Field Data Under Climate Change Scenarios

Understanding wave changes under climate change requires the integration of historical wave data and future scenario projections (Mentaschi et al., 2017; Lemos et al., 2023; Meucci et al., 2023). Historical data elucidate seasonal variations and long-term trends, while future scenarios provide critical insights into potential wave changes under various climate assumptions. Together, these datasets are essential for assessing risks and developing climate adaptation strategies. This study analyses extreme wave height data from the Northwest Pacific over the past 60 years and estimates design wave heights for different return periods.

The Coupled Model Intercomparison Project (CMIP) coordinates global climate modelling experiments, enabling a multi-model framework to understand past, present, and future climate variability. CMIP6, the latest phase, integrates data from 1850 to 2014 into various models to produce projections from 2015 to 2100. The CMIP6 dataset is hosted on the Earth System Grid Federation (ESGF), a unified platform for storing, retrieving, and sharing results from global climate models. This platform supports climate simulation validation, predictive modelling, and policy formulation. Among the CMIP6 models, the EC-Earth3 model, developed by the EC-Earth consortium, has demonstrated superior performance in simulating atmospheric circulation over East Asia (Döscher et al., 2022; Zheng et al., 2022). EC-Earth3 provides high-resolution wind speed and sea-level pressure data under five SSP scenarios: SSP1-1.9, SSP1-2.6, SSP2-4.5, SSP3-7.0, and SSP5-8.5. These datasets span from 2015 to 2100, with a spatial resolution of 100 km and a temporal resolution of 3 hours. Additionally, historical data (1850–2014) with identical resolutions are available.

For this study, the horizontal and vertical wind speed components were selected from the SSP5-8.5 high-emission scenario using the experimental configuration r1i1p1f1 as the driving force for subsequent wave simulations. This configuration accounts for simulation ensemble number (r1), initial conditions (i1), model physics (p1), and forcing signal (f1), as summarized in Tab. 1. Wind speed data under this scenario were input into the WAVEWATCH III model to simulate wave dynamics.

https://doi.org/10.5194/egusphere-2024-3954
Preprint. Discussion started: 3 February 2025

Table 1: Number of Model Configurations for Each EC-Earth3 Scenario.

Emission Scenario	Very Low Emission SSP1-1.9	Low Emission SSP1-2.6	Moderate Emission SSP2-4.5	High Emission SSP3-7.0	Very High Emission SSP5-8.5
Experimental Configuration	r4i1p1f1 r5i1p1f1	r1i1p1f1 r4i1p1f1 r5i1p1f1 r6i1p1f1 r8i1p1f1 r9i1p1f1 r11i1p1f1 r13i1p1f1 r15i1p1f1	r1i1p1f1 r4i1p1f1 r5i1p1f1 r6i1p1f1 r9i1p1f1 r11i1p1f1 r13i1p1f1	r1i1p1f1 r4i1p1f1 r5i1p1f1 r6i1p1f1 r9i1p1f1 r11i1p1f1 r13i1p1f1	r1i1p1f1 r4i1p1f1 r5i1p1f1 r6i1p1f1 r9i1p1f1 r11i1p1f1 r13i1p1f1
Number of Experimental Configurations	2	9	8	8	8

3.2 Historical Wave Simulation in the Northwest Pacific (1961–2020)

Wave simulations were conducted using the WAVEWATCH III model, a third-generation wave model based on the WAM framework (WAMDI, 1998; Komen et al., 1994). Developed by Tolman (1997, 1999) at NOAA/NCEP, WAVEWATCH III has advanced to version 6.07 (WW3DG, 2019), which was employed in this study. The model uses the wave action density balance equation to solve the frequency-direction spectrum, as described by Equation (1):

$$\frac{\partial N}{\partial t} + \nabla_x \cdot \dot{\vec{x}}\, N + \frac{\partial}{\partial k}\dot{k}N + \frac{\partial}{\partial \theta}\dot{\theta}N = \frac{S}{\sigma}, \quad (1)$$

where N is the wave action density spectrum, a function of wave number k, direction θ, position vector x, and time t; S represents the net effect of sources and sinks; and σ denotes the intrinsic frequency, or relative frequency, which is the wave frequency relative to the mean flow of local ocean currents.

The model operates under two assumptions: (i) implicit integration, allowing wave fields to evolve over spatial and temporal scales significantly larger than those of individual waves; and (ii) parameterization of physical mechanisms, which limits accurate simulations in areas with abrupt bathymetric changes, making the model more suitable for regions with stable seabed topography. Based on these assumptions, WAVEWATCH III is applied to grid scales larger than 1–10 km and areas outside the wave breaking. The model outputs wave spectra at each grid point, which are used to calculate significant wave height, wave period, and other statistical wave parameters.

This study used EC-Earth3 wind field data to drive the WAVEWATCH III model, with bathymetric inputs derived from ETOPO1, a global terrain dataset from the National Geophysical Data Center. The wave model resolutions—100 km spatially and 3 hours temporally—align with those of the EC-Earth3 climate model. Monthly mean wave heights were calculated from simulation results to assess regional wave characteristics.

https://doi.org/10.5194/egusphere-2024-3954
Preprint. Discussion started: 3 February 2025

Monthly mean wave heights were calculated based on the simulation results, and the findings are presented in Figs. 1 to 4. The analysis of wave height time series reveals distinct characteristics across the four regions studied:

1. Taiwan Strait: Wave heights in this region are relatively low, ranging from 0.5 m to 1.5 m, with occasional peaks approaching 2 m. The overall wave energy is minimal, and a slight downward trend in wave heights is evident.
2. Eastern Waters of Taiwan: This region exhibits significantly higher wave heights, with peaks exceeding 2 m on a near-monthly basis. The high wave intensity is primarily attributed to the region's exposure to the open Pacific Ocean. Despite this, a slight declining trend in wave heights is observed.
3. Northern Waters of Taiwan: Wave height variations in the northern waters are comparable to those in the Taiwan Strait, fluctuating between 0.5 m and 1.5 m. However, the amplitudes and frequencies of fluctuations are marginally higher.
4. Southern Waters of Taiwan: Wave heights in the southern waters are moderately higher than those in the Taiwan Strait, with a broader fluctuation range and occasional peaks reaching 2.5 m. A slight declining trend in wave heights is also apparent.

Overall, the eastern waters of Taiwan exhibit the highest wave intensity, reflecting their exposure to open ocean dynamics, whereas the Taiwan Strait is characterized by the most stable conditions. The southern and northern waters of Taiwan demonstrate intermediate wave intensities. Notably, all regions exhibit a declining trend in wave heights over the past 60 years. These findings underscore the critical importance of long-term wave monitoring and modelling to inform the design and risk assessment of coastal and marine infrastructure.

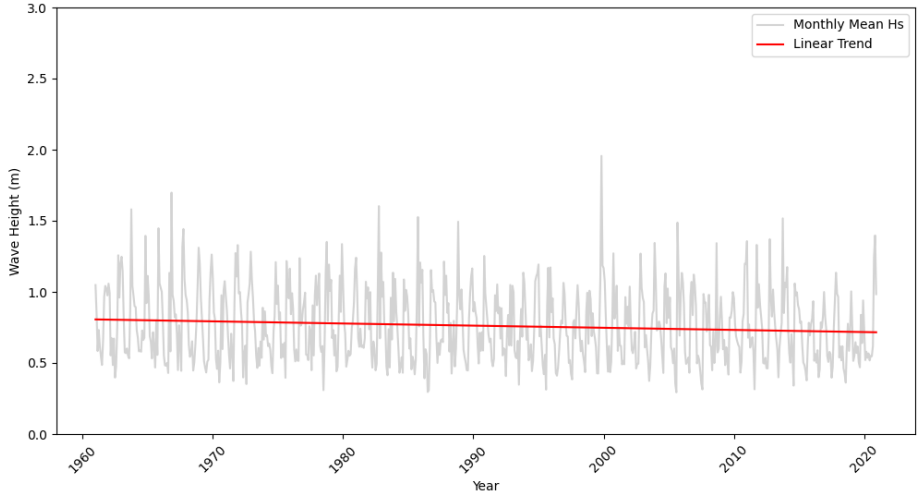

Figure 1: Time Series of Mean Wave Height Variations in the Taiwan Strait (1961–2020).

https://doi.org/10.5194/egusphere-2024-3954
Preprint. Discussion started: 3 February 2025

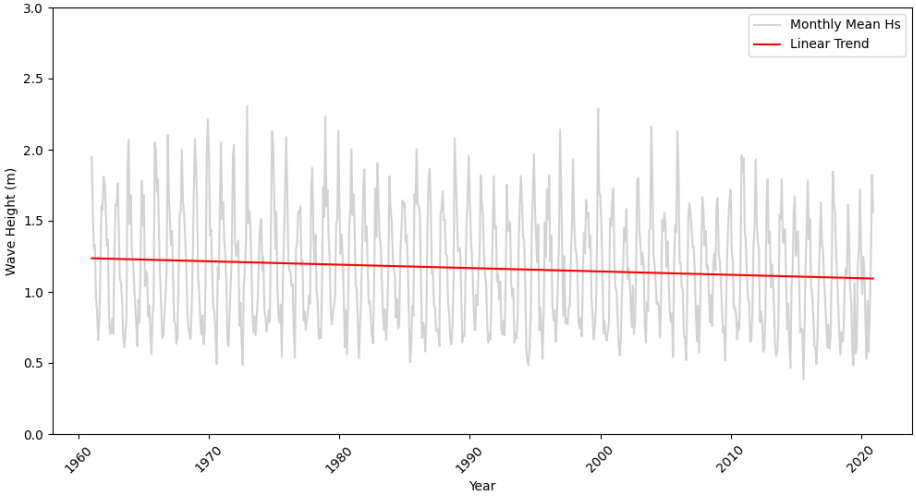

Figure 2: Time Series of Mean Wave Height Variations in the Eastern Waters of Taiwan (1961–2020).

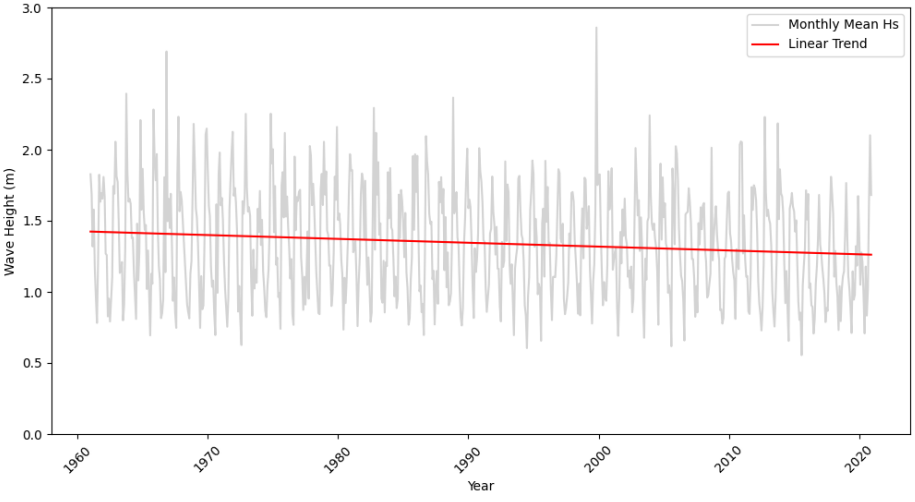

135

Figure 3: Time Series of Mean Wave Height Variations in the Northern Waters of Taiwan (1961–2020).

https://doi.org/10.5194/egusphere-2024-3954
Preprint. Discussion started: 3 February 2025

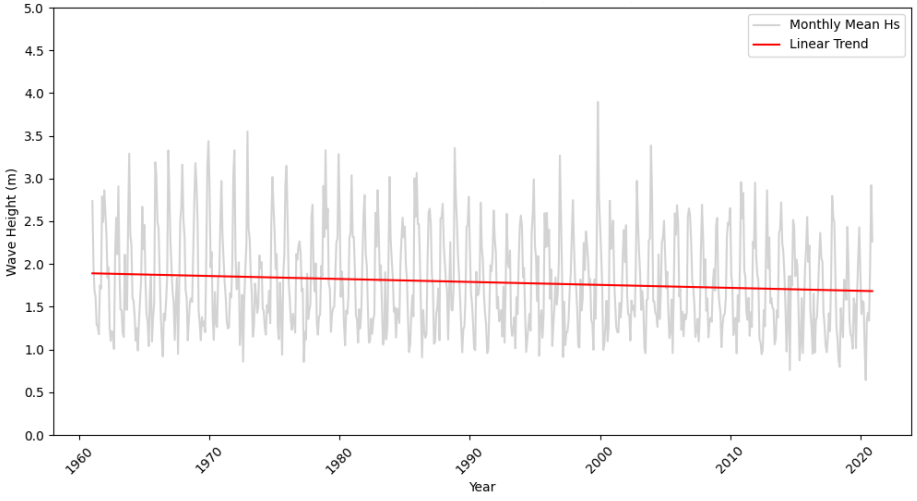

Figure 4: Time Series of Mean Wave Height Variations in the Southern Waters of Taiwan (1961–2020).

4 Methodology

4.1 Artificial Intelligence-Based Wave Downscaling Model

Modern climate models, despite advancements in resolution and physical complexity, still lack the ability to provide high-resolution regional climate data for smaller grid areas. To address this limitation, downscaling methods are critical for generating high-resolution spatial and temporal wave data. These methods enable a more precise representation of future changes in coastal wave conditions, enhancing the reliability of climate change impact assessments.

Artificial Intelligence (AI) offers a robust framework for improving wave simulations by mimicking human-like cognitive functions such as learning and decision-making. AI encompasses a range of methodologies, including machine learning and deep learning, which are particularly effective at processing large and complex datasets. Deep learning, a subfield of machine learning, employs multi-layered neural networks to autonomously identify features in raw data, eliminating the need for manual feature extraction. This study employs deep learning as a statistical downscaling method to enhance wave simulation resolution and reliability. Among deep learning architectures, Convolutional Neural Networks (CNNs) are effective for extracting spatial features, while Recurrent Neural Networks (RNNs) excel at capturing temporal dependencies. By integrating these two approaches, this study utilizes a Convolutional Recurrent Neural Network (CRNN) to refine the spatial resolution of wave simulations from 100 km to 3 km and the temporal resolution from 3 hours to 1 hour. The CRNN architecture is illustrated in Fig. 5.

The CNN component captures spatial features using convolutional layers, which extract patterns from input data, and pooling layers, which reduce feature map dimensions to enhance computational efficiency. These processes are defined by the following equations:

https://doi.org/10.5194/egusphere-2024-3954
Preprint. Discussion started: 3 February 2025

$$C_{i,j} = Conv\left(X_{i,j}, j, W_c\right) + b_c, \tag{2}$$

$$P_{i,j} = Pool\left(C_{i,j}\right), \tag{3}$$

where $C_{i,j}$ represents the output of the convolutional layer, $X_{i,j}$ is the low-resolution input data, W_c is the convolution kernel, and b_c is the bias term of the convolutional layer.

The RNN component processes the temporal sequence features to capture dependencies over time, defined as:

$$H_{i,j} = \mathrm{RNN}\left(P_{i,j}, h_0\right), \tag{4}$$

To enhance resolution, the CRNN model employs a deconvolution layer for upsampling, increasing feature map dimensions and transforming low-resolution features into high-resolution representations:

$$U = Upsample(H), \tag{5}$$

Finally, a mapping operation projects low-resolution wave data into high-resolution wave data:

$$Y = Map(U), \tag{6}$$

To evaluate the CRNN model's performance, multiple statistical metrics were employed, including Root Mean Square Error (RMSE), Pearson Correlation Coefficient (ρ), and Scatter Index (SI). RMSE quantifies the overall error magnitude, calculated as:

$$\mathrm{RMSE} = \sqrt{\frac{\sum_{i=1}^{n}(T_i - P_i)^2}{n}}, \tag{7}$$

where T and P represent observed and predicted significant wave heights, respectively, and n is the number of time steps.

The Pearson Correlation Coefficient measures the linear relationship between observed and predicted values:

$$\rho = \frac{\sum_{i=1}^{n}(T_i - \overline{T})(P_i - \overline{P})}{\sqrt{\sum_{i=1}^{n}(T_i - \overline{T})^2}\sqrt{\sum_{i=1}^{n}(P_i - \overline{P})^2}}, \tag{8}$$

where $\overline{T}$ and $\overline{P}$ are the mean values of the observed and predicted datasets.

The SI normalizes prediction errors relative to observed values to quantify scatter plot dispersion:

$$SI = \frac{\sqrt{\frac{\sum_{i=1}^{n}\left[(T_i - \overline{T})(P_i - \overline{P})\right]^2}{n}}}{\overline{T}}, \tag{9}$$

Extreme event predictions were evaluated using RMSE for errors exceeding the 95th percentile:

$$\mathrm{ERR}_{\mathrm{ABS}} = |T - P|, \tag{10}$$

$$\mathrm{RMSEQ}_{95} = \sqrt{\frac{\sum_{i \in (\mathrm{ERA}_{\mathrm{ABS}} > 95\text{th percentile of } \mathrm{ERA}_{\mathrm{ABS}})}(\mathrm{ERA}_{\mathrm{ABS}})^2}{n}}, \tag{11}$$

https://doi.org/10.5194/egusphere-2024-3954
Preprint. Discussion started: 3 February 2025

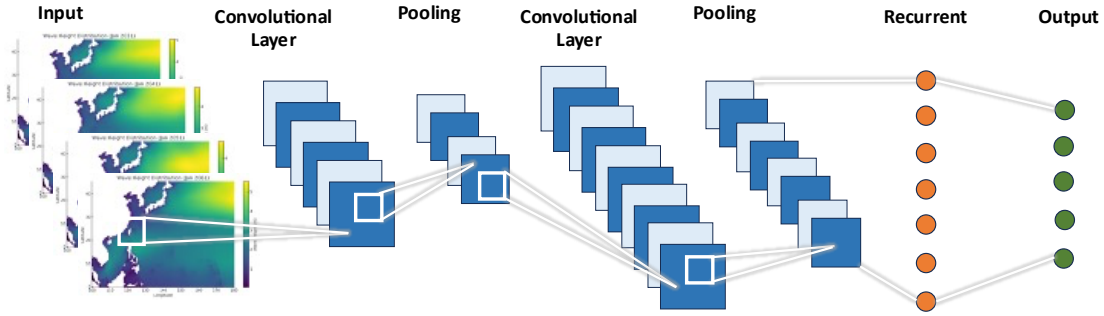

Figure 5: Architecture of the Convolutional Recurrent Neural Network (CRNN).

4.2 Generalized Pareto Distribution (GPD) for Return Period Calculation Based on Extreme Value Theory

To analyse extreme wave behaviour, this study identified extreme wave events exceeding the 95th percentile of the simulated wave height data (1961–2020). The Generalized Pareto Distribution (GPD) was used to model these events, as it effectively characterizes the distribution tails associated with extreme values. The GPD is defined as:

$$F(y) = 1 - (1 + \frac{\xi y}{\sigma})^{-1/\xi}, \quad (12)$$

where y=x-u, u is the threshold (95th percentile), ξ is the shape parameter, and σ is the scale parameter.

Using the GPD model, wave heights for return periods (T) of 10, 25, 50, 75, 100, and 200 years were estimated:

$$T = \frac{1}{1-F(x)}, \quad (13)$$

where $F(x)$ is the cumulative probability corresponding of wave height x.

Uncertainty in return period estimates was quantified using the Bootstrap resampling method. Resampled datasets were used to fit the GPD and calculate wave heights, yielding mean values and 95% confidence intervals for different return periods. This approach ensures robust evaluation of design wave heights under extreme conditions.

5 Analysis and Discussion of Design Wave Heights Across Return Periods

Design wave heights are critical parameters in evaluating the risks associated with ocean and coastal structures over various timescales. They determine the ability of these structures to withstand extreme wave events, ensuring long-term stability and safety. The typhoon season (May to October) is recognized as the primary source of extreme wave events in the Northwest Pacific, with strong winds and rapid typhoon movements generating extreme waves over short periods. These waves pose significant threats to offshore facilities, coastlines, and port infrastructure. Analysing design wave heights exclusively from annual wave data risks underestimating the actual threats posed during the typhoon season. To address this, the study focuses on wave simulation data from the typhoon seasons of 1961–2020, calculating design wave heights for return periods of 10, 25, 50, 75, 100, and 200 years.

https://doi.org/10.5194/egusphere-2024-3954
Preprint. Discussion started: 3 February 2025

The results, illustrated in Fig. 6, reveal a consistent increase in extreme wave heights with longer return periods. For the 10-year return period, design wave heights are concentrated between 20° N to 40° N latitude and 120° E to 160° E longitude, generally ranging from 10 m to 15 m. During this period, wave conditions remain relatively stable, with lower wave heights near Taiwan. For the 25-year return period, significant increases in wave heights are observed, particularly in typhoon-prone regions, where wave heights often exceed 20 m.

Wave heights in the southern and eastern waters of Taiwan are notably higher due to their exposure to the open Pacific Ocean, the influence of the Kuroshio Current, and strong typhoon-induced wind fields. These factors lead to greater wave energy, contrasting with the Taiwan Strait, where enclosed geography and monsoonal influences result in relatively stable wave height variations. As the return periods extend to 50 and 75 years, the increasing trend in design wave heights becomes even more pronounced, especially in the southern and eastern waters of Taiwan, where wave heights exceed 25 m and approach 30 m in some areas. These trends highlight the escalating intensity and frequency of extreme wave events, imposing stricter requirements on the design of marine and coastal structures in these regions.

Further analysis for 100-year and 200-year return periods reveals that parts of the Northwest Pacific, particularly between 20° N to 30° N latitude and 120° E to 160° E longitude, experience dramatic wave height increases, with values nearing 30 m. These findings underscore the growing impact of extreme wave conditions as return periods lengthen. For regions like the southern and eastern waters of Taiwan, the need for enhanced resilience in marine and coastal infrastructure is paramount. These regions, frequently affected by typhoons, demand stronger monitoring, risk management, and disaster prevention measures to address the challenges posed by intensifying wave conditions.

To refine the spatial analysis, the waters surrounding Taiwan were divided into four regions: the Taiwan Strait (22° N to 26° N, 118° E to 121° E), the eastern waters of Taiwan (22° N to 26° N, 121° E to 125° E), the northern waters of Taiwan (26° N to 28° N, 118° E to 122° E), and the southern waters of Taiwan (20° N to 22° N, 118° E to 121° E). Table 2 presents the design wave heights calculated for each region during the typhoon season.

In the Taiwan Strait, design wave heights increase from 3.54 m for the 10-year return period to 5.19 m for the 200-year return period. The eastern waters of Taiwan exhibit a rise from 4.42 m to 4.92 m over the same period. The northern waters of Taiwan demonstrate a smaller increase, from 3.71 m to 3.98 m. Notably, the southern waters of Taiwan show the largest increase, with wave heights growing from 3.59 m to 6.44 m. This substantial increase in the southern waters underscores the higher vulnerability of this region to extreme wave events during typhoon seasons.

Wave heights in the western waters of Taiwan remain relatively stable, ranging between 10 m and 20 m, with limited increases as return periods extend. This stability can be attributed to reduced exposure to typhoon impacts. However, the potential influence of typhoon circulations and waves originating from the South China Sea necessitates regular assessments, even for these relatively low-risk areas.

In summary, the study highlights distinct regional variations in design wave heights, emphasizing the heightened risk in the southern and eastern waters of Taiwan. These findings provide critical scientific insights for the design, planning, and risk assessment of marine and coastal infrastructure, particularly in regions prone to extreme wave conditions. As return periods

https://doi.org/10.5194/egusphere-2024-3954
Preprint. Discussion started: 3 February 2025

lengthen, the observed trends underscore the urgency of integrating these projections into infrastructure resilience and disaster preparedness strategies.

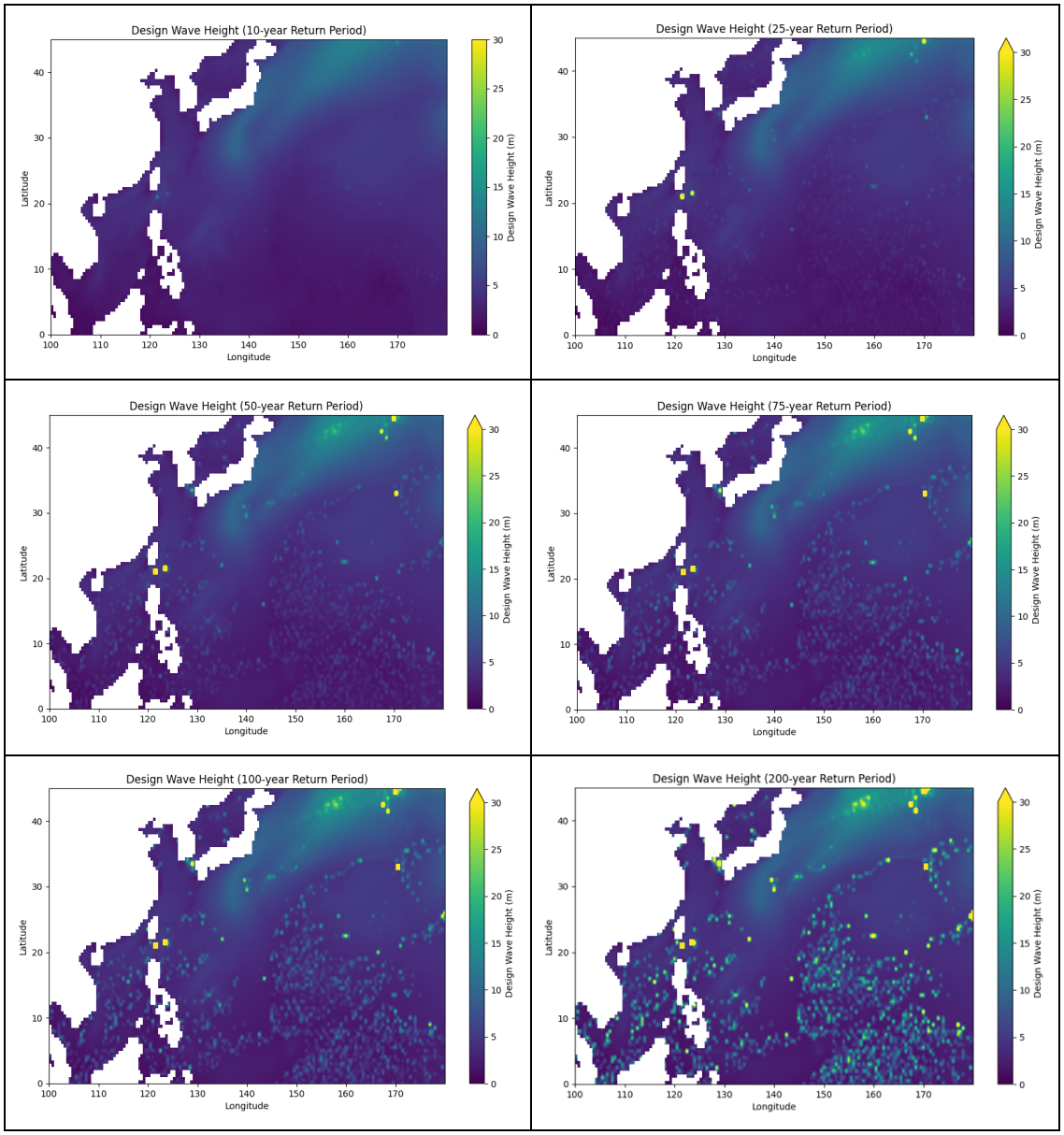

Figure 6: Typhoon Season Design Wave Heights for the Northwest Pacific under 10-Year, 25-Year, 50-Year, 75-Year, 100-Year, and 200-Year Return Periods (Arranged Left to Right, Top to Bottom).

https://doi.org/10.5194/egusphere-2024-3954
Preprint. Discussion started: 3 February 2025

Table 2: Design Wave Heights During Typhoon Season Across Different Return Periods for Each Region.

Return Period / Design Wave Heights (m) / Region	10-year	25-year	50-year	75-year	100-year	200-year
Taiwan Strait	3.54	3.71	3.93	4.15	4.36	5.19
Eastern Taiwan Waters	4.42	4.50	4.57	4.64	4.70	4.92
Northern Taiwan Waters	3.71	3.76	3.81	3.84	3.88	3.98
Sourthern Taiwan Waters	3.59	3.85	4.24	4.61	4.98	6.44

6 Conclusions

This study investigates the spatial and temporal characteristics of extreme wave heights in the Northwest Pacific, focusing on the waters surrounding Taiwan. Using high-resolution wave simulations and statistical analysis, the results provide critical insights into the design wave heights across return periods during the typhoon season (May to October). The findings highlight the increasing risks posed by extreme wave events and the need for adaptive strategies in coastal and marine infrastructure design.

The analysis reveals that extreme wave heights increase significantly with longer return periods. In the southern and eastern waters of Taiwan, design wave heights exceed 25 m and approach 30 m for the 200-year return period. These regions, exposed to the open Pacific Ocean, frequent typhoons, and the Kuroshio Current, exhibit the highest wave intensities. In contrast, the Taiwan Strait is characterized by relatively stable wave conditions due to its enclosed geography and dominance of monsoonal influences. However, periodic assessments remain essential even in these regions to account for potential risks from typhoon-induced waves.

The study emphasizes the importance of integrating design wave heights based on extended return periods into the planning and construction of coastal and offshore structures. This approach is crucial for ensuring that such structures can withstand increasingly severe oceanographic conditions under future climate scenarios. Furthermore, these results provide a robust scientific foundation to support decision-making processes in infrastructure planning and disaster risk reduction. Policymakers and engineers should prioritize incorporating these findings into adaptive design frameworks, particularly for offshore facilities in typhoon-prone regions such as the eastern waters of Taiwan.

By employing artificial intelligence-based downscaling methods, this study achieves high-resolution wave simulations and enhances the predictive capabilities for assessing extreme wave events. The framework developed here serves as a critical tool for understanding wave behaviours under various climate scenarios. It also contributes to improving the accuracy and reliability of wave modelling, offering a valuable reference for managing risks associated with extreme wave conditions in the Northwest Pacific.

https://doi.org/10.5194/egusphere-2024-3954
Preprint. Discussion started: 3 February 2025

Competing interests

The author declares that he has no conflict of interest.

Acknowledgements

The author would like to thank financial support from National Science and Technology Council (NSTC 112-2625-M-006-008-).

References

Aarnes, O. J., M. Reistad, Ø. Breivik, E. Bitner-Gregersen, L. I. Eide, O. Gramstad, A. K. Magnusson, B. Natvig, E. Vanem (2017), Projected changes in significant wave height toward the end of the 21st century: Northeast Atlantic. J. Geophys. Res. Oceans, 122, 3394–3403, J. Geophys. Res. Oceans, 120, 2973-2992, doi:10.1002/2014JC010565.

Chellapilla, K., M. Shilman, P. Simard (2006), Combining multiple classifiers for faster optical character recognition. Document Analysis Systems Vii, Proceedings 3872, 358-367.

Chien, H. H.-Y. Cheng, and M.-D. Chiou (2014), Wave climate variability of Taiwan waters. J Oceanogr 70, 133–152, https://doi.org/10.1007/s10872-014-0218-8.

Dobrynin, M., J. Murawsky, and S. Yang (2012), Evolution of the global wind wave climate in CMIP5 experiments. Geophys. Res. Lett., 39, L18606, doi:10.1029/2012GL052843.

Erikson, L. H., C. Hegermiller, P. Barnard, P. Ruggiero, and M. van Ormondt (2015), Projected wave conditions in the eastern north pacific under the influence of two CMIP5 climate scenarios. Ocean Modell., 96, 171–185, doi:10.1016/j.ocemod.2015.07.004.

Fan, Y., and S. M. Griffies (2014), Impacts of parameterized Langmuir turbulence and nonbreaking wave mixing in global climate simulations. J. Clim., 27(12), 4752–4775, doi:10.1175/JCLI-D-13-00583.1.

Fan, Y., I. M. Held, S.-J. Lin, and X. L. Wang (2013), Ocean warming effect on surface gravity wave climate change for the end of the twenty-first century. J. Clim., 26(16), 6046–6066, doi:10.1175/JCLI-D-12-00410.1.

Gallagher, S., E. Gleeson, R. Tiron, R. McGrath, and F. Dias (2016), Wave climate projections for Ireland for the end of the 21st century includ- ing analysis of EC-Earth winds over the North Atlantic Ocean. Int. J. Climatol., 36(14), 4592–4607, doi:10.1002/joc.4656.

Grabemann, I., N. Groll, J. Mo€ller, and R. Weisse (2015), Climate change impact on North Sea wave conditions: A consistent analysis of ten projections. Ocean Dyn., 65(2), 255–267, doi:10.1007/s10236-014-0800-z.

Hemer, M. A., and C. E. Trenham (2016), Evaluation of a CMIP5 derived dynamical global wind wave climate model ensemble. Ocean Modell., 103, 190–203, doi:10.1016/j.ocemod.2015.10.009.

https://doi.org/10.5194/egusphere-2024-3954
Preprint. Discussion started: 3 February 2025

Hemer, M. A., Y. Fan, N. Mori, A. Semedo, and X. L. Wang (2013), Projected changes in wave climate from a multi-model ensemble. Nat. Clim. Change, 3(5), 471–476, doi:10.1038/nclimate1791.

Hinkel, J., and Coauthors (2021), Uncertainty and bias in global to regional scale assessments of current and future coastal flood risk. Earth's Future, 9, e2020EF001882, https://doi.org/10. 1029/2020EF001882.

Khon, V., I. Mokhov, F. Pogarskiy, A. Babanin, K. Dethloff, A. Rinke, and H. Matthes (2014), Wave heights in the 21st century Arctic Ocean simulated with a regional climate model. Geophys. Res. Lett., 41, 2956–2961, doi:10.1002/2014GL059847.

Kirezci, E., I. R. Young, R. Ranasinghe, S. Muis, R. J. Nicholls, D. Lincke, and J. Hinkel (2020), Projections of global-scale extreme sea levels and resulting episodic coastal flooding over the 21st century. Sci. Rep., 10, 11629, https://doi.org/10.1038/s41598-020-67736-6.

Komen, G. J., L. Cavaleri, M. Donelan, K. Hasselmann, S. Hasselmann, and P. E. A. M. Janssen (1994), Dynamics and modelling of ocean waves. Cambridge University Press, 532 pp.

Le Cun, Y., B. Boser, J. S. Denker, D. Henderson, R. E. Howard, W. Hubbard, L.D. Jackel (1989), Backpropagation Applied to Handwritten Zip Code Recognition. Neural Computation 1 (4), 541-551.

Lemos, G., A. Semedo, R. Kumar, M. Dobrynin, A. Akpinar, B. Kamranzad, J. Bidlot, H. Lobeto (2023), Performance evaluation of a global CMIP6 single forcing, multi wave model ensemble of wave climate simulations. Ocean Modelling, 184, 1–21, Ocean Modelling, 103, 177-189, doi:10.1016/j.ocemod.2016.02.006.

Marcos, M., J. Rohmer, M. I. Vousdoukas, L. Mentaschi, G. L. Cozannet, and A. Amores (2019), Increased extreme coastal water levels due to the combined action of storm aurges and wind waves. Geophysical Research Letters, 46, 4356–4364. https://doi.org/ 10.1029/2019GL082599

Martınez-Asensio, A., M. Marcos, M. N. Tsimplis, G. Jorda, X. Feng, and D. Gomis (2016), On the ability of statistical wind-wave models to capture the variability and long-term trends of the North Atlantic winter wave climate. Ocean Modelling, 103, 177–189, doi:10.1016/j.ocemod.2016.02.006.

Mentaschi, L., M. I. Vousdoukas, E. Voukouvalas, A. Dosio, and L. Feyen (2017), Global changes of extreme coastal wave energy fluxes triggered by intensified teleconnection patterns. Geophys. Res. Lett., 44, 2416–2426, https://doi.org/10.1002/2016GL072488.

Meucci, A., I. R. Young, M. Hemer, C. Trehnam, and I. G. Watterson (2023), 140 Years of Global Ocean Wind-Wave Climate Derived from CMIP6 ACCESS-CM2 and EC-Earth3 GCMs: Global Trends, Regional Changes, and Future Projections. Journal of Climate, 36, 6, 1605-1631, doi: https://doi.org/10.1175/JCLI-D-21-0929.1

Mori, N., T. Shimura, T. Yasuda, and H. Mase (2013), Multi-model climate projections of ocean surface variables under different climate scenarios—Future change of waves, sea level and wind. Ocean Eng., 71, 122–129, doi:10.1016/j.oceaneng.2013.02.016.

Perez, J., M. Menendez, P. Camus, F. J. Mendez, and I. J. Losada (2015), Statistical multi-model climate projections of surface ocean waves in Europe. Ocean Modell., 96, 161–170, doi:10.1016/j.ocemod.2015.06.001.

https://doi.org/10.5194/egusphere-2024-3954
Preprint. Discussion started: 3 February 2025

Semedo, A., R. Weisse, A. Behrens, A. Sterl, L. Bengtsson, and H. Guenther (2012), Projection of global wave climate change toward the end of the twenty-first century. J. Clim., 26(21), 8269–8288, doi:10.1175/JCLI-D-12-00658.1.

Shimura, T., N. Mori, and M. A. Hemer (2016), Variability and future decreases in winter wave heights in the western North Pacific. Geophys. Res. Lett., 43, 2716–2722, doi:10.1002/2016GL067924.

Shimura, T., N. Mori, and H. Mase (2015a), Future projections of extreme ocean wave climates and the relation to tropical cyclones: Ensemble experiments of MRI-AGCM3.2H. J. Clim., 28(24), 9838–9856, doi:10.1175/JCLI-D-14-00711.1.

Shimura, T., N. Mori, and H. Mase (2015b), Future projection of ocean wave climate: Analysis of SST impacts on wave climate changes in the western North Pacific. J. Clim., 28(8), 3171–3190, doi:10.1175/JCLI-D-14-00187.1.

Tolman, H. L. (1997), User manual and system documentation of WAVEWATCH-III version 1.15. NOAA / NWS / NCEP / OMB Technical Note 151, 97 pp.

Tolman, H. L. (1999), User manual and system documentation of WAVEWATCH-III version 1.18. NOAA / NWS / NCEP / OMB Technical Note 166, 110 pp.

Wang, X. L., Y. Feng, and V. R. Swail (2015), Climate change signal and uncertainty in CMIP5-based projections of global ocean surface wave heights. J. Geophys. Res. Oceans, 120, 3859–3871, doi:10.1002/2015JC010699.

Wang, X. L., Y. Feng, and V. R. Swail (2014), Changes in global ocean wave heights as projected using multimodel CMIP5 simulations. Geophys. Res. Lett., 41, 1026–1034, doi:10.1002/2013GL058650.

WAMDIG (1988), The WAM model – a third generation ocean wave prediction model. J. Phys. Oceanogr., 18, 1775–1809.

Ministry of Science and Technology (MOST) (2022), Highlights of Scientific Findings in the IPCC Sixth Assessment Report on "Impacts, Adaptation, and Vulnerability" and Updated Assessment of Climate Change Impacts in Taiwan.

Ministry of Science and Technology (MOST), Research Center for Environmental Changes, Academia Sinica, Central Weather Administration, Department of Earth Sciences, National Taiwan Normal University, and National Science and Technology Center for Disaster Reduction (2021), Highlights of Scientific Findings in the IPCC Sixth Assessment Report and Updated Assessment of Climate Change Impacts in Taiwan.